Caving 2026 – A van As, D Cumming-Potvin & J Wesseloo (eds)

doi:10.36487/ACG_repo/2645_91

Drawpoint spacing in block/panel caving

Raúl Castro [a,b], **René Gómez** [b,c,*]

[a] *Department of Mining Engineering, University of Chile, Chile*

[b] *Laboratory of Block Caving, Advanced Mining Technology Centre, Chile*

[c] *Faculty of Engineering, Universidad de Concepción, Chile*

Abstract

The design of the production level depends directly on the layout of drawpoints which must be configured primarily to ensure both level stability and high productivity. In recent years, an increase in drawpoint spacing has been observed, driven mainly by the need for greater stability and reduced development times and costs. However, design methodologies have not evolved at the same pace, resulting in a gap between traditional approaches and the conditions encountered in primary rock at the greater depths where most modern caving operations are now developed. To address this gap, the present study proposes a new drawpoint spacing design methodology that incorporates the knowledge and insights generated in block and panel caving over the past decade including physical modelling, simulations and observations of markers at the field. The methodology presented here provides an updated and practical design tool aligned with the geological and operational environments characteristic of contemporary caving mines.

Keywords: *block caving, gravity flow, underground mine design*

1 Introduction

Block and panel caving are increasingly applied to deeper orebodies in competent rock masses, where high in situ stresses and large extraction heights define the current operating environment. Under these conditions, extraction level design faces significant challenges associated with coarse fragmentation, limited caveability, and the need for preconditioning to facilitate cave initiation and propagation. In addition, increasing ore column heights amplify stress concentrations and influence both flow behaviour and drawpoint performance (Carreño et al. 2025; Cuello & Newcombe 2018; Paredes 2022). These factors introduce complex interactions between geomechanics and granular flow, making the design of extraction layouts – particularly drawpoint spacing and drift configuration – more critical and less amenable to traditional empirical approaches.

The extraction level constitutes the primary interface between the caved rock mass and the production system, and its design is governed by the configuration of drawpoints, production drifts, and overall layout geometry. Common layouts, such as the El Teniente and Henderson configurations, define the spatial arrangement and interaction of drawpoints, with drawpoint spacing increasing in recent deep-level operations to accommodate higher stresses and larger equipment (Flores 2014; Paredes 2022). These design choices directly influence the gravity flow of fragmented material, affecting flow uniformity, draw control, and ultimately ore recovery and dilution. In addition, the layout influences the development and redistribution of stresses within the broken material during ore draw (Castro et al. 2020; Pierce 2019) which, in turn, affects flow behaviour and drawpoint interaction. As a result, extraction layout design plays a critical role in balancing flow performance with geomechanical response within the caved column under increasingly demanding mining conditions.

[*] Corresponding author. Email address: regomez@udec.cl

The performance of the extraction level is inherently controlled by the coupling between fragmentation, gravity-driven flow, and cave propagation (Castro et al. 2025; Fuenzalida et al. 2018; Karekal et al. 2011). In particular, coarse fragmentation – commonly observed in competent, hard rock masses, even with the application of preconditioning – can significantly alter flow behaviour by promoting more irregular flow near to drawbells, increased variability in drawpoint interaction, and a higher propensity for flow interruptions such as hang-ups. Under these conditions, wider drawpoint spacing may be feasible, as flow zones can extend and interact over larger distances; however, this may also lead to less uniform draw and increased uncertainty in recovery. Despite these effects, existing empirical design guidelines have been largely developed for finer fragmentation conditions (Laubscher 2000; Laubscher et al. 2017; Laubscher 1994) and may not be directly applicable to these environments, highlighting the need for improved understanding and more robust design methodologies.

Extraction level design has traditionally relied on a combination of empirical and semi-empirical approaches developed from field observations, physical modelling, and operational experience, as reflected in the work of Castro et al. (2012), Laubscher et al. (2017), Laubscher (1994), Susaeta (2004), Trueman et al. (2008), and others. These methodologies define key design parameters such as drawpoint spacing, commonly derived from conceptual or analytical representations of flow zones, including kinematic models that describe the movement of fragmented material toward drawpoints. In this context, parameters such as the draw angle are used to estimate the extent of drawpoint interaction and the geometry of flow zones (Castro et al. 2012). Additional design considerations include drift orientation and layout geometry to facilitate efficient material handling, as well as drawbell geometry to promote controlled initiation of flow. While these approaches have provided a practical basis for design, they are generally founded on simplified representations of flow behaviour and fragmentation conditions, with limited capability to explicitly account for the complex interactions observed in modern deep, hard rock caving environments (Brunton et al. 2016).

Table 1 presents a summary of representative block and panel caving operations, including production layout dimensions and approximate mining depths. The information highlights the significant depths currently achieved by caving mines worldwide and provides context for the production level layouts commonly adopted in deep caving operations. Recent experience from deep caving operations has highlighted a trend toward coarser fragmentation (Hurtado et al. 2007; Ngidi et al. 2010; Srikant et al. 2004) that directly influences flow behaviour and drawpoint interaction. Although numerous studies have explored these effects through mine-scale observations, as well as numerical and physical modelling, their outcomes have remained largely case-specific and have not been consolidated into generalised design criteria. As a result, extraction level design continues to rely on empirical rules that do not explicitly incorporate the influence of coarse fragmentation or the associated changes in flow and cave response. This lack of updated design guidance underscores the need to integrate current understanding into more robust and transferable design methodologies.

This study aims to develop a design methodology for the extraction level in block and panel caving operations under current mining conditions. The proposed approach integrates knowledge obtained from recent mine-scale observations, physical modelling, and advanced numerical simulations, including the discrete element method and cellular automata-based tools. By incorporating the effects of coarse fragmentation and its interaction with flow behaviour and cave response, the methodology seeks to provide a more robust basis for defining key design parameters, including drawpoint spacing and layout configuration. In doing so, this work contributes toward bridging the gap between current understanding and practical design criteria for modern caving environments.

Table 1 Production level layout in block caving (Batkhuu 2025; Brown et al. 2022; Castro et al. 2012; Liu et al. 2020; Parsons et al. 2024; Sahupala et al. 2010; Stegman et al. 2022; Wilson et al. 2016)

Mine	Drawpoint layout type	Spacing (m × m)	Depth (m)
Northparkes (E26) lift 1	Herringbone	30 × 16	900
Northparkes (E26) lift 2	Herringbone	30 × 18	900
Northparkes E48	Herringbone/El Teniente	30 × 18	581
Northparkes E22	El Teniente	30 × 18	–
PC1 Cadia Valley	El Teniente	32 × 20	1200–1,450
DOZ	Herringbone	30 × 18	1,200
DMLZ	El Teniente	30 × 20	1,700
Palabora	Herringbone	34 × 17	1,650
El Teniente – Teniente 4 Sur	El Teniente	30 × 17	550–660
El Teniente – Esmeralda B2	El Teniente	30 × 15	600–800
El Teniente – Reno	El Teniente	30 × 20	830
El Teniente – D. Regimiento	El Teniente	34 × 20	600
El Teniente - Diamante	El Teniente	30 × 20	800–1,000
Henderson	Herringbone	31 × 17	1,550
Oyu Tolgoi - Hugo North Lift 1	El Teniente	28 × 15	1,300
Chuquicamata UG lift 1	El Teniente	32 × 24/30 × 22	200–900
New Afton	El Teniente	27 × 16.5	1,150
Pulang Copper mine	Herringbone	30 × 15	300–500

2 Methodology

The methodology proposed in this study for defining the extraction level design is primarily based on determining the drawpoint spacing based on rock fragmentation and operational criteria. This spacing is established to maximise the stability of the production level while ensuring the interaction and connectivity of flow zones, thereby enhancing reserve recovery. Based on current knowledge, particle size distribution is recognised as a key parameter controlling the geometry of the flow zones. Accordingly, the fragmentation within the draw column is first characterised and subsequently used to define the main design parameters.

Additionally, it is considered that ore extraction leads to a continuous increase in the height and width of the drawzone, particularly under coarse fragmentation conditions. It is also well established that the growth of these zones follows a consistent relationship, as illustrated in Figure 1 based on various reported measurements. Notably, the data reported by Laubscher (1994) indicate a lower rate of isolated movement zone (IMZ) width expansion compared to more recent studies.

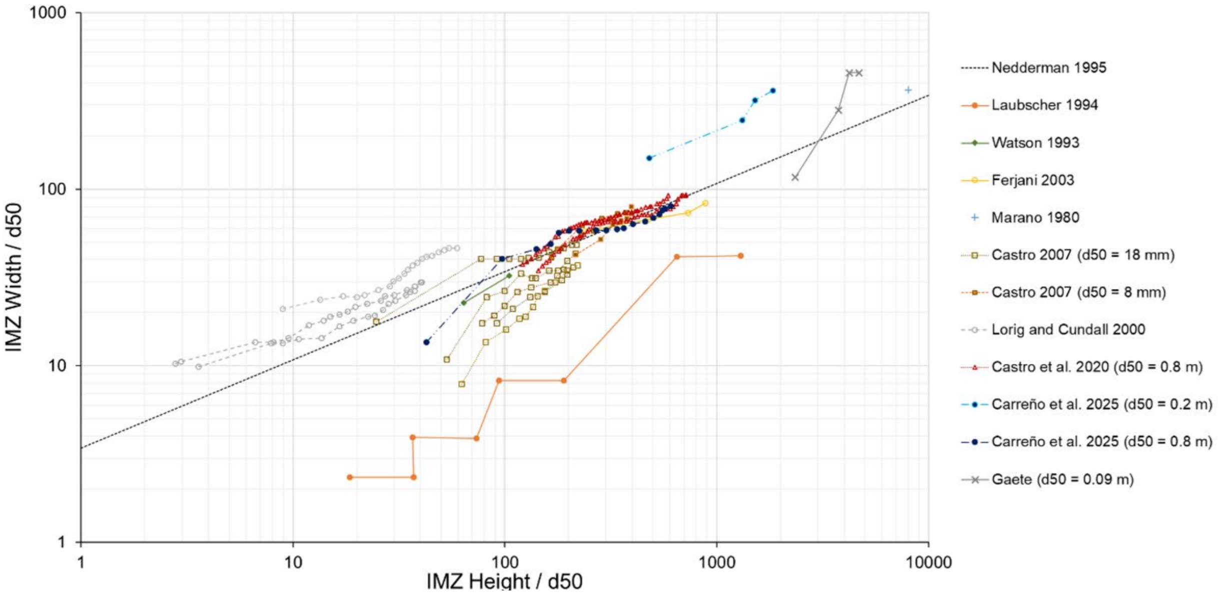

Figure 1 Summary of the height-to-width geometry relationship from several gravity flow studies in cave mining. Mean sizes (d_{50}) are reported at the mine-scale, except for Castro (2007) (Carreño et al. 2025; Castro 2007; Castro et al. 2020; Ferjani 2003; Gaete 2026; Laubscher 1994; Lorig & Cundall 2000; Marano 1980; Nedderman 1995; Pierce 2010; Watson 1993)

2.1 Rock fragmentation prediction

In block/panel caving mining, 3 stages of fragmentation are typically identified (in situ, primary, and secondary; Brown 2007a), which collectively control the resulting fragment size distribution as extraction progresses. For early-stage engineering assessments, the Laubscher method (Laubscher 2000a, 2000b) can be used to estimate fragmentation. Although several approaches exist to evaluate both in situ and primary fragmentation (e.g. Eadie 2003; Paluszny & Zimmerman 2017; Rogers et al. 2010), this method is widely recognised for being rapid and straightforward to apply while incorporating a key parameter: the rock mass rating (RMR).

Despite being originally proposed several decades ago, the method has been revisited in this study to reflect the evolution of caving mining conditions. In particular, it has been updated using more recent fragmentation data, especially for more competent rock masses and in operations where preconditioning techniques are applied.

2.1.1 In situ and primary fragmentation

To determine the in situ fragmentation, the original Laubscher methodology is applied using Table 2 (Laubscher 2000a). The procedure requires first estimating the proportion of the rock mass within each RMR class (from 1 to 5). Subsequently, a weighted sum is performed for each size interval to obtain the percentage of the rock size distribution corresponding to that interval. For example, if the rock mass consists of 70% with RMR class 1 and 30% with RMR class 2, the in situ fragmentation for the 0.5–1.0 m rock size interval is calculated as (5 × 70% + 12.5 × 30%).

Table 2 Fractions of size intervals assigned to each rock mass rating (Laubscher 2000a)

Rock size (m)	1	2	3 A	3B	4	5
<0.5	0	2.5	7.5	15	27.5	80
0.5–1.0	5	12.5	20	42.5	52.5	15
1.0–2.0	10	27.5	32.5	25	15	5
2.0–4.0	40	35	27.5	12.5	5	0
4.0–8.0	30	15	10	5	0	–
8.0–16.0	10	5	2.5	0	–	–
>16.0	5	2.5	0	–	–	–

Once the in situ fragmentation has been defined as a function of the RMR distribution within the rock mass, the primary fragmentation can be estimated. To this end, Laubscher proposed the use of the caving stress factor, β. This parameter represents the effect of induced stresses on the cave-back (Equation 1):

$$\beta(\%) = 100\% - 2\big(\%RMR(C5)\big) - \big(\%RMR(C4)\big) - 0.5\big(\%RMR(C3B)\big) - R \tag{1}$$

where:

β = caving stress factor (%)

RMR = rock mass rating, expressed here as the proportion of rock mass within each RMR class

R = originally a reduction factor accounting for the presence of geological structures.

In Equation 1, a value of 5% is recommended for *R* in zones where hydraulic fracturing (HF) has been applied. If intensive dynamic de-stress blasting (DDE) has also been implemented, a higher value (up to 30%) is recommended, based on some studies (Calderon 2023; Castro et al. 2024; Gómez et al. 2023).

Once the caving stress factor has been determined, Table 3 is used to define the proportion of each size interval that remains within the same interval and the proportion that fragments into smaller size intervals. For example, considering resulting size interval (0.5–1.0 m), 25β% fragments from original interval (1.0–2.0 m) are transferred to interval (0.5–1.0 m), while 10β% fragments from original interval (1.0–2.0 m) are transferred to interval (0.5–1.0 m). Consequently, the remaining (100–10β)% stays within interval (0.5–1.0 m) while 10β% from original interval (1.0–2.0 m) are transferred to the lower size interval. The reduction is applied as a function of the caving stress factor (Equation 1). It should be noted that this approach assumes that, at most, a given size interval fragments into the immediately lower interval. Future work could extend this assumption to allow redistribution across all smaller size intervals, as considered in some comminution models (Austin & Concha 1994; Gómez et al. 2017; Merino 1986).

Table 3 Fragmentation balance between the different intervals determined by stress caving

Rock size (m)	Resulting rock size (%)						
In situ	**<0.5**	**0.5–1.0**	**1.0–2.0**	**2.0–4.0**	**4.0–8.0**	**8.0–16.0**	**>16.0**
<0.5	100	–	–	–	–	–	–
0.5–1.0	10β	100–10β	–	–	–	–	–
1.0–2.0	–	25β	100–25β	–	–	–	–
2.0–4.0	–	10β	50β	100 - 60β	–	–	–
4.0–8.0	–	–	30β	60β	100–90β	–	–
8.0–16.0	–	–	–	50β	50β	100–100β	–
>16.0	–	–	–	–	70β	30β	100–100β

To facilitate the calculation of the resulting primary fragmentation, Table 4 can be used. This table summarises the mass fractions that must be added to or subtracted from each size interval, accounting for both the fragmentation occurring within each interval and the fragments received from larger size intervals. In Table 4, Ωi is the mass fraction of the *ith* size interval, while *fij* is the fraction transferred from *i* to *j* size interval. *fij* are obtained from Table 3.

Table 4 Guide table for determining primary fragmentation based on the stress caving criterion

Rock size (m)	In situ distribution	Primary distribution
<0.5	Ω_1	$\Omega_1 + f_{21}\,\Omega_2$
0.5–1.0	Ω_2	$(1 - f_{21})\,\Omega_2 + f_{32}\,\Omega_3 + f_{42}\,\Omega_4$
1.0–2.0	Ω_3	$(1 - f_{32})\,\Omega_3 + f_{43}\,\Omega_4 + f_{53}\,\Omega_5$
2.0–4.0	Ω_4	$(1 - f_{42} - f_{43})\,\Omega_4 + f_{54}\,\Omega_5 + f_{64}\,\Omega_6$
4.0–8.0	Ω_5	$(1 - f_{53} - f_{54})\,\Omega_5 + f_{65}\,\Omega_6 + f_{75}\,\Omega_7$
8.0–16.0	Ω_6	$(1 - f_{64} - f_{65})\,\Omega_6 + f_{76}\,\Omega_7$
>16.0	Ω_7	$(1 - f_{75} - f_{76})\,\Omega_7$
Total	$\sum_{i=1}^{7} \Omega_i = 100\%$	$\Omega_1 + f_{21}\,\Omega_2 + (1 - f_{21})\,\Omega_2 + f_{32}\,\Omega_3 + \ldots = 100\%$

In this way, the resulting primary fragmentation can be determined as a function of the proportion that each size interval loses (transferred to smaller intervals) and the proportion it gains from larger rock sizes. If a higher level of detail is required, particularly to distinguish the undercut zone affected by blasting, the fragmentation at the drawbell and undercut levels can be defined using available fragmentation models (Hekmat et al. 2024; Lopez et al. 2017; Onederra 2004) or specialised tools (Vivero et al. 2024).

2.1.2 Secondary fragmentation

Once the primary fragmentation has been defined, it is used as an input parameter to estimate secondary fragmentation. A straightforward approach is to continue applying the Laubscher methodology (Laubscher 2000b) or other available models (Dorador 2016; Golder 2012; Gómez et al. 2021; Pierce et al. 2010). However, since secondary fragmentation is intrinsically linked to gravitational flow, this study employs a secondary fragmentation model embedded within a flow simulation framework (Castro et al. 2024; Gómez et al. 2025). This model applies a reduction to the characteristic size, *x*, using Equation 2:

$$Rx = \alpha_1 (\frac{\sigma_v}{UCS})^{\alpha_2} + \left(\frac{\gamma\delta}{\sigma_v}\right)^{\alpha_3} \quad (2)$$

where:

Rx	=	reduction in the characteristic particle size x (cm), per unit distance travelled (m). Consequently, Rx has units of cm/m
α_1, α_2, and α_3	=	fitting constants
σ_v	=	average vertical stress within the broken material column induced by the overburden (MPa)
UCS	=	uniaxial compressive strength (MPa).

The parameter γ is the shear strain which is a dimensionless quantity related to the interaction height and the width of the shear band (Pierce 2010). The parameter δ is associated with system friction and is a calibrated, dimensionless value. In addition, the flow simulator (based on a cellular automata approach) incorporates a travel distance, t_d, defined as the minimum distance a cell must move for the size reduction R_x to be applied, and a minimum size, d_{min}, corresponding to the smallest size to which a rock fragment can be reduced. Although these parameters are user-defined, values on the order of 10 and 0.1 m are recommended for t_d and d_{min}, respectively.

2.2 Isolate movement zone

Once the fragmentation has been estimated, the geometry of the flow zones can be defined. To determine the spacing between drawpoints, it is first necessary to estimate the width of the IMZ (IMZ_w). Subsequently, the graph presented in Figure 2 is applied, whereby the IMZ_w is estimated as a function of the mean fragment size (d_{50}) and the tonnage extracted from the drawpoint. This figure was constructed using data compiled from various gravity flow studies in caving environments (Armijo et al. 2014; Carreño et al. 2025; Castro et al. 2020; Gaete 2026; Le-Feaux et al. 2021; Vasquez 2026).

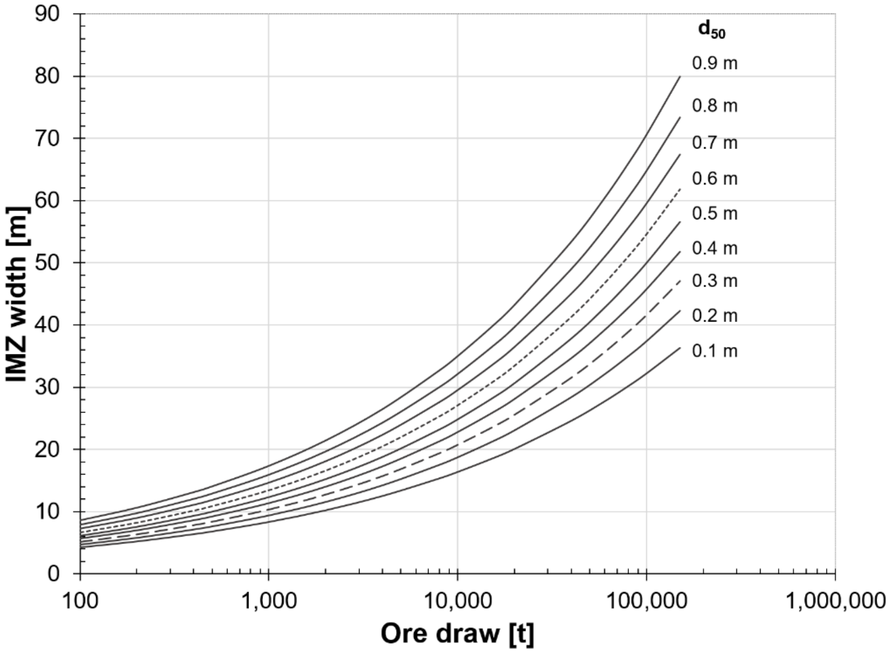

Figure 2 Graph used to determine the width of the isolated movement zone as a function of the extracted mass. The lines within the graph represent the mean fragment size (d_{50}) of the estimated fragmentation

As an example, if an assuming an extraction rate of 0.2 t/m²·d and an preliminary extraction layout of 34 × 24 m, the area associated with a drawpoint is 408 m² (corresponding to half of the drawbell area). The cumulative tonnage extracted after one month of production would be per Equation 3:

$$Ore\ draw\ [t] = 30\ [d] \cdot 0.2 \left[{}^{t}\!/_{m^2 d}\right] \cdot 408[m^2] = 2{,}448\ t \tag{3}$$

For the cumulative tonnage considered and an estimated d_{50} of 0.3 m, the relationship shown in Figure 2 results in an IMZ_w of approximately 14 m. The calculation can then be iteratively updated as the final layout parameters become available. Nevertheless, a key operational consideration at this stage is the selection of the extraction rate, since it governs the expected time to interaction and eventual connection between neighbouring drawpoints. For example, to minimise load transfer through the fragmented material, prolonged interruptions in extraction should be avoided, and the undercut material should be drawn in a timely manner (Brown 2007b). This effect may vary depending on the undercutting strategy employed (Batkhuu et al. 2024; Butcher 2000).

2.3 Drawpoint spacing

Once the fragmentation and the width of the movement zones have been estimated, the next step is to define the extraction layout dimensions. For this purpose, it is also necessary to account for the dimensions of the loader equipment (load-haul-dump; LHD) to be used or evaluated, as these directly influence the determination of the extraction drift length. To define the production level design, an iterative process is carried out considering different equipment options that meet the required production capacity. The LHD size must be selected to achieve the target productivity, which strongly depends on bucket capacity. For design purposes, the equipment width and length are required parameters, as they are used to define the drift width and the extraction drift length, respectively.

For the cross-section width, there must be at least 75 cm of clearance between the equipment and the drift walls. Similarly, for the cross-section height, a minimum clearance of 75 cm is required. Considering these definitions together with additional clearance factors, it is possible to determine the extraction drift length and slope parameters for these units, using Equation 4

$$L_{ED} = L_E + L_S - W_{PDH} \tag{4}$$

where:

L_{ED} = extraction drift length (m)

L_E = LHD length (m)

L_S = slope material length (m)

W_{PDH} = production drift width (m; parallel to the extraction drift).

These distances can be seen in Figure 3.

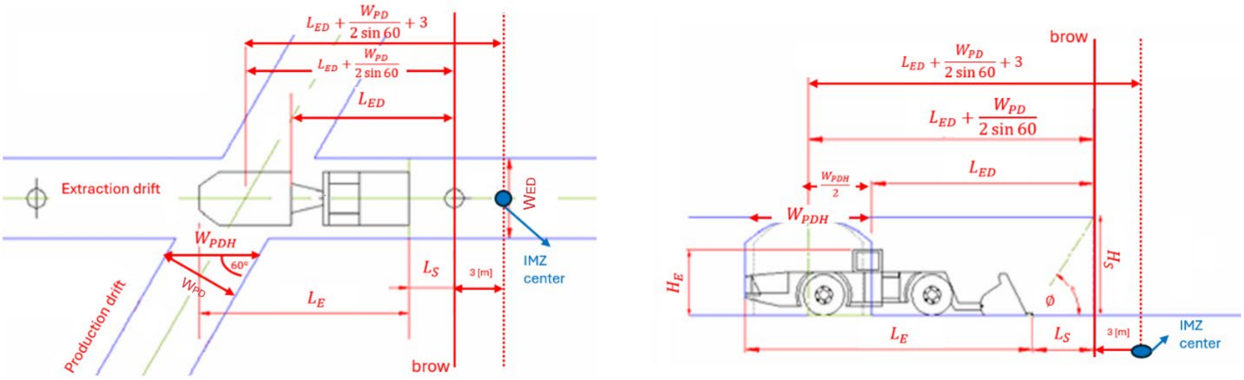

(a) (b)

Figure 3 Geometries considered for defining extraction level distances, including equipment dimensions. (a) Plan view; (b) Profile view

The 3 horizontal metres to the right of the LHD is an approximation that represents the centre of the isolated extraction ellipsoid, slightly displaced from the drawpoint. The slope length (L_s) is calculated using trigonometric relationships (Equation 5):

$$L_S = \frac{H_S}{tan(\phi)} \tag{5}$$

where:

Hs = drawpoint height

ϕ = angle of repose of the muck pile.

Similarly, the horizontal production width (distance parallel to the extraction drift) is calculated as follows (Equation 6):

$$W_{PDH} = \frac{W_{PD}}{sin(60)} \tag{6}$$

The longest distance between production drifts, $L_{MAX,PD}$ (diagonal distance, green line in Figure 4) is calculated (Equation 7):

$$L_{MAX,PD} = 2 \cdot L_{ED} + L_{DB} + W_{PDH} \tag{7}$$

Here, the drawbell length (L_{DB}) is a predefined parameter, typically ranging between 10 and 14 m. Future studies may be conducted to analyse changes in this distance. In this case, a value of 14 m is adopted, although it may vary depending on design considerations ($L_{DB} < IMZw$). Based on this the perpendicular distance between production drifts (D_{PD}) can be calculated using Equation 8. These distances are shown in Figure 4.

$$D_{PD} = L_{MAX,PD} \cdot sin(60) \tag{8}$$

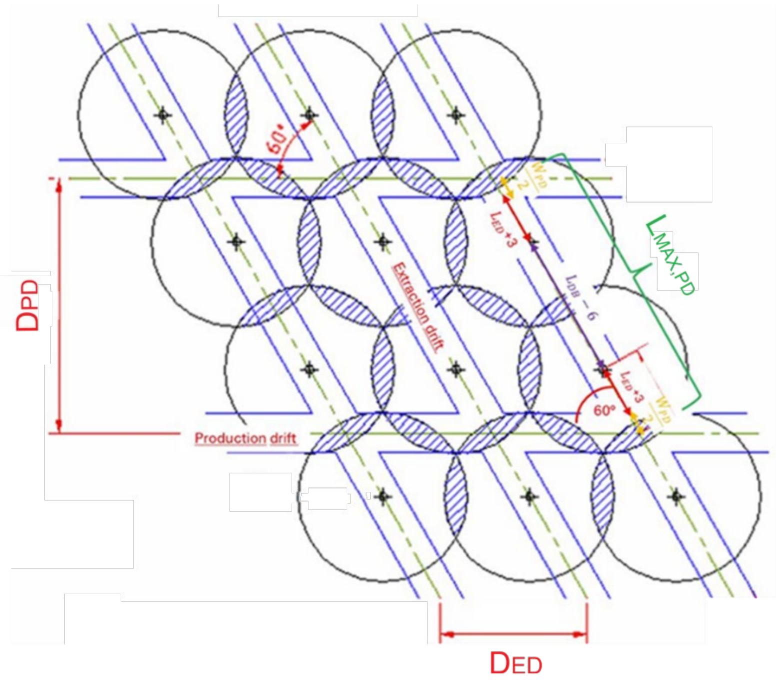

Figure 4 Plan view of the distances between production and extraction drifts to be determined

Then, the distance between extraction drifts (D_{ED}), orientated parallel to the production drifts, must be determined based on the following criteria (Equation 9):

$$D \leq IMZ_W \tag{9}$$

where:

D = distance between the centres of two neighbouring ellipsoids

IMZ_W = IMZ diameter (or width).

This distance criteria can be seen in Figure 5a. In Figure 5a, a movement ellipsoid interacts with 6 other IMZs; however, the analysis focuses only on its interaction with the ellipsoids whose distances are denoted as L_1, L_2, and L_3, due to symmetry. The largest of these distances is L_1, which therefore should be taken as D. This distance satisfies the previous inequality, as overlap exists between the ellipsoids, meaning that it is smaller than the IMZ width. An example that does not satisfy the previous inequality is shown in Figure 5b.

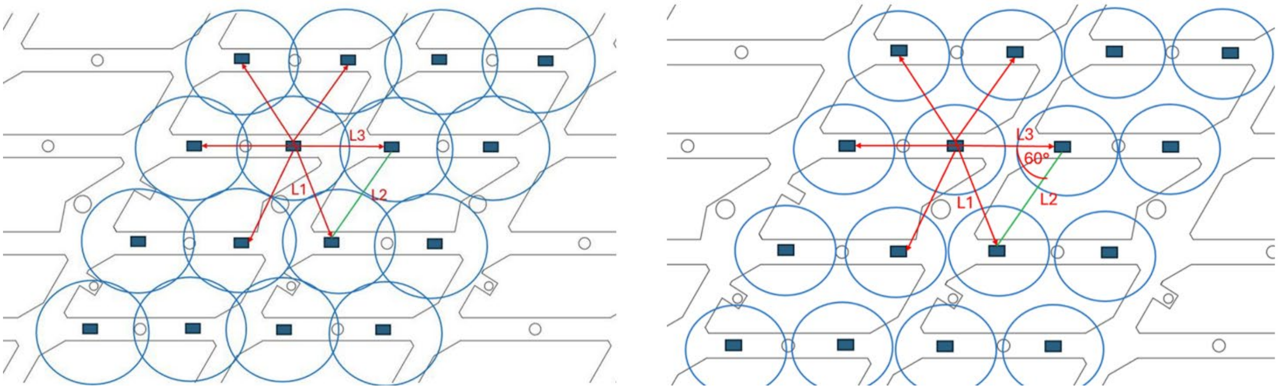

(a) (b)

Figure 5 Plan view of the diameters of the isolated movement ellipsoids projected onto a El Teniente-type layout. (a) Diameters of the IMZs at each drawpoint interacting; (b) Diameters of each drawpoint without achieving interaction

Note that L_3 is defined in terms of L_{ED} and W_{PDH}, as indicated in Equation 10:

$$L_3 = 2(L_{ED}) + W_{PDH} \tag{10}$$

In Figure 5b, L_1 is greater than IMZ_W; therefore, the previous inequality (Equation 9) is no longer satisfied and no interaction occurs between the IMZs. The analysis then focuses on calculating distance L_2, which represents the spacing between the extraction drift (parallel) and the production drift (D_{ED}). This distance can be determined using the law of cosines, as the angle between L_2 and L_3 is 60° (Figure 5), as defined by the layout geometry. Accordingly, Equation 11 is obtained:

$$(L_1)^2 = (L_2)^2 + (L_3)^2 - 2 \cdot L_2 \cdot L_3 \cdot cos(60) \tag{11}$$

This results in a quadratic equation, where L_2 is the unknown variable, while L_1 (IMZ_w) is an input parameter. Solving the equation yields 2 solutions: one positive and one negative. Since a physical distance is being calculated, only the positive solution is considered.

3 Results and discussions

This section presents an example application of the design methodology introduced in Section 2. For this purpose, parameters typically used in block/panel caving mining are considered. A predefined finer fragmentation is assumed (d_{50} = 0.7 m), and a Sandvik LH621i LHD unit is used as a reference. This equipment has a width of 3.2 m, a length of 12.5 m, and a height to the canopy of 2.9 m. Based on these dimensions, and using the equations presented in Section 2.3, a production drift width of 4.7 m, and a minimum production drift height of 3.7 m are obtained. Additionally, considering a slope height of 3.5 m and an ore angle of repose of 50°, a slope length of 2.9 m is derived. A drawbell length of 14 m is selected, which should provide a larger pillar.

The IMZ_w is determined using Figure 2. Assuming a d_{50} of 0.7 m, an IMZ_w of 24 m is obtained after 4,800 t of extracted material. Based on the assumed geometry, this can be achieved in less than 2 months. With these dimensions, the maximum distance between production drifts, $L_{MAX,PD}$, is 39.4 m (Equation 7), D_{PD} is 34.2 m (Equation 8), L_1 is 24 m, and L_3 is 25.4 m (Equation 10)

Subsequently, using the previously defined distances and solving Equation 11 for L_2 (D_{ED}), a distance of 22.2 m is obtained. Based on these values, and adopting a El Teniente-type layout, a 34 × 24 m layout is defined, as it is comparable to the well-established 32 × 20 m layout. The resulting layout dimensions are shown in Figure 6.

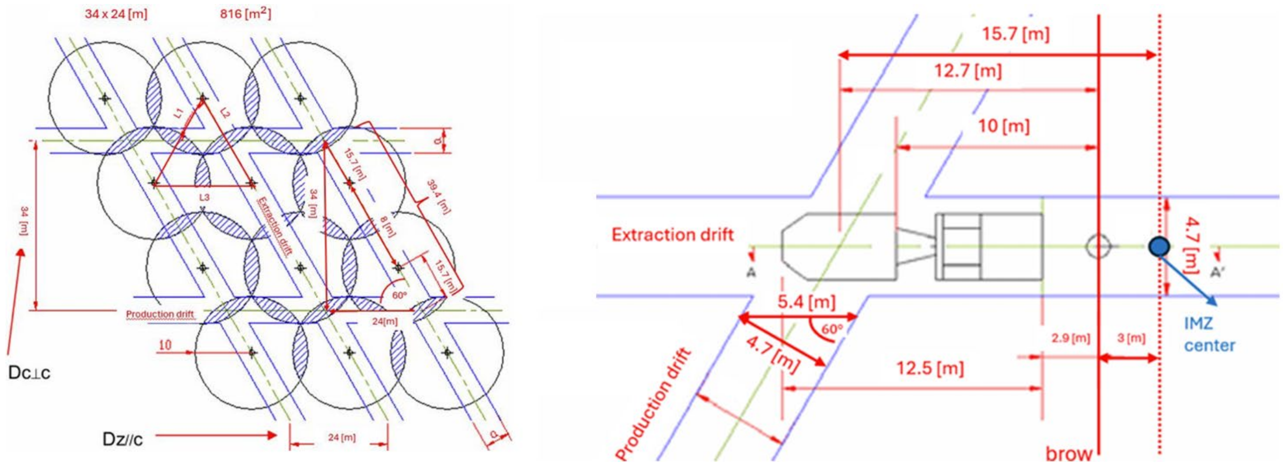

(a) (b)

Figure 6 Plan view of the diameters of the El Teniente-type layout. (a) Diameters of the IMSs at each drawpoint interacting; (b) Diameters of each drawpoint without achieving interaction

Finally, by incorporating into the design the extraction ellipsoids previously defined, it becomes evident that overlap occurs among all ellipsoids associated with each drawpoint in the El Teniente-type layout. Figure 7 illustrates the ellipsoid diameters at an IMZ height of 50 m, corresponding to approximately 2,000 t of extracted material. A good overlap is observed between the characteristic distances (L_1, L_2, and L_3), which is expected to ensure favourable extraction conditions.

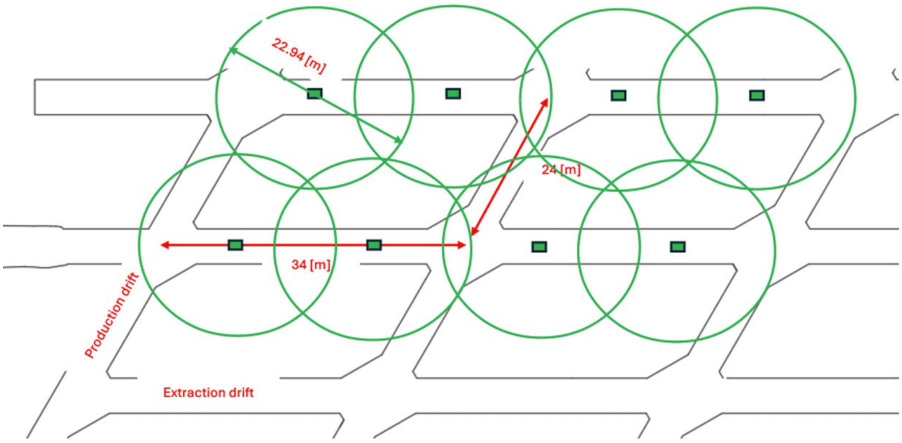

Figure 7 Schematic representation of the movement zone with an IMZ width of 22.94 m and an extraction grid of 34 × 24 m

4 Conclusion

This study presents a design methodology for the extraction level layout in block and panel caving operations, integrating fragmentation assessment, flow zone geometry, and equipment constraints into a coherent framework. A key aspect of the methodology is the accurate estimation of rock fragmentation, as it directly controls the development of movement zones and, consequently, the design criteria adopted in subsequent stages.

The results highlight that both fragmentation and equipment selection (LHD) are critical parameters in defining an appropriate extraction layout. Fragmentation influences the size and interaction of flow zones, while equipment dimensions govern drift geometry and spacing. Together, these factors determine the optimal configuration of the extraction grid, as well as the criteria related to connection heights and extraction timing required to ensure proper flow interaction and operational performance.

Finally, this work provides an updated and practical design methodology for extraction layouts in block and panel caving, contributing to improved decision-making under current mining conditions characterised by greater depths, higher stresses, and increasing productivity demands.

Acknowledgement

This paper/work was (partially) funded by the CONICYT/PIA Project CIA250010. R. Gomez thanks FONDECYT Iniciacion 11240668.

References

Armijo, F, Irribarra, S & Castro, R 2014, 'Experimental study of fines migration for caving mines', in R Castro (ed.), *Proceedings of the 3rd International Symposium on Block and Sublevel Caving*, Universidad de Chile, Santiago, pp. 356–362.

Austin, L & Concha, F 1994, *Diseño y Simulación de Circuitos de Molienda y Clasificación* (Design and Simulation of Comminution and Classification Circuits), CYTED.

Batkhuu, B 2025, *Operational Benchmaring and Ground Response Analysis for Undercutting in High-Stress Cave Mines*, Master's thesis, The University of Queensland, Brisbane.

Batkhuu, B, van As, A & Lett, J 2024, 'Evolution of undercutting in panel and block caves', in Daniel Johansson & Håkan Schunnesson (eds), *MassMin 2024: Proceedings of the International Conference & Exhibition on Mass Mining*, Luleå University of Technology, Luleå, pp. 1593–1610, https://doi.org/10.36487/ACG_repo/2435_R-07

Brown, ET 2007a, 'Fragmentation assessment', *Block Caving Geomechanics*, Julius Kruttschnitt Mineral Research Centre, Indooroopilly, pp. 184–228.

Brown, ET 2007b, 'Cave initation by undercutting', *Block Caving Geomechanics*, Julius Kruttschnitt Mineral Research Centre, Indooroopilly, pp. 229–287.

Brown, K, Webster, S, Bruning, T, Garcia, O & Campbell, AD 2022, 'An iterative design and schedule approach to the E22 block cave project and production planning at CMOC Northparkes Mines: a case study', in Y Potvin (ed.), *Caving 2022: Proceedings of the Fifth International Conference on Block and Sublevel Caving*, Australian Centre for Geomechanics, Perth, pp. 303–314, https://doi.org/10.36487/ACG_repo/2205_20

Brunton, I, Lett, G & Sharrock, G 2016, 'Full-scale Flow markers experiments at Ridgeway Deeps and Cadia east cave operations', *Massmin 2016: Seventh International Conference & Exhibition on Mass Mining*, Australasian Institute of Mining and Metallurgy, Melbourne, pp. 817–824.

Butcher, RJ 2000, 'Block cave undercutting - aims, strategies, methods and management', *Proceedings of Massmin 2000*, Australasian Institute of Mining and Metallurgy, Melbourne, pp. 423–428.

Calderon, O 2023, *Validación y Calibración del Modelo de Fragmentación Secundaria Aplicado en Flowsim BC* (Validation and Calibration of the Secondary Fragmentation Model Implemented in Flowsim BC), Universidad de Concepcion, Concepción.

Carreño, N, Castro, R, Gómez, R & Segovia, C 2025, 'Physical modeling of high extraction columns in block cave mining', *International Journal of Rock Mechanics and Mining Science*, vol. 192, no. 106140, https://doi.org/10.1016/j.ijrmms.2025.106140

Castro, R 2007, *Study of the Mechanisms of Gravity Flow for Block Caving*, PhD thesis, The University of Queensland, Brisbane.

Castro, R, Gómez, R, Castillo, JJ & Jerez, O 2024, 'Fragmentation model integrated in a gravity flow simulator for block caving planning', *Granular Matter*, vol. 26, no. 1, pp. 20–22, https://doi.org/10.1007/s10035-024-01396-5

Castro, R, Gómez, R, Pierce, M & Canales, J 2020, 'Experimental quantification of vertical stresses during gravity flow in block caving', *International Journal of Rock Mechanics and Mining Sciences*, vol. 127, no. 104237, https://doi.org/10.1016/j.ijrmms.2020.104237

Castro, RL, Vargas, R & De La Huerta, F 2012, 'Determination of drawpoint spacing in panel caving: A case study at the El Teniente mine', *Journal of the Southern African Institute of Mining and Metallurgy*, vol. 112, no. 10, pp. 871–876.

Castro, R, Oyarzo, D, Gomez, R, Suzuki, K & Cifuentes, M 2025, 'Coupling geomechanical and gravity flow models to obtain more representative flow simulations and air-gap risk identification in caving mining', *International Journal for Numerical and Analytical Methods in Geomechanics*, vol. 49, no. 1, pp. 376–390, https://doi.org/doi.org/10.1002/nag.3880

Cuello, D & Newcombe, G 2018, 'Key geotechnical knowledge and practical mine planning guidelines in deep, high-stress, hard rock conditions for block and panel cave mining', in Y Potvin & J Jakubec (eds), *Caving 2018: Proceedings of the Fourth International Symposium on Block and Sublevel Caving*, Australian Centre for Geomechanics, Perth, pp. 17–36, https://doi.org/10.36487/ACG_rep/1815_0.2_Cuello

Dorador, L 2016, *Experimental Investigation of the effect of Broken ore Properties on Secondary Fragmentation During Block Caving,* PhD thesis, The University of British Columbia, Vancouver.

Eadie, B 2003, *A Framework for Modelling Fragmentation in Block Caving*, PhD thesis, The University of Queensland, Brisbane.

Ferjani, M 2003, *An Investigation of the Plug/Funnel-Flow Model*, PhD thesis, University of Minnesota, Minneapolis.

Flores, G 2014, 'Future challenges and why cave mining must change', in R Castro (ed.), *Proceedings of the 3rd International Symposium on Block and Sublevel Caving*, Universidad de Chile, Santiago, pp. 23–52.

Fuenzalida, MA, Pierce, ME & Katsaga, T 2018, 'REBOP–FLAC3D hybrid approach to cave modelling', in Y Potvin & J Jakubec (eds), *Caving 2018: Proceedings of the Fourth International Symposium on Block and Sublevel Caving*, Australian Centre for Geomechanics, Perth, pp. 297–312, https://doi.org/10.36487/ACG_rep/1815_20_Pierce

Gaete, M 2026, *Modelamiento Fisico de Flujo Gravitacional en Columnas de Extraccion Altas* (Physical Modeling of Gravity Flow in High Extraction Columns), Universidad de Concepcion, Concepcion.

Golder Associates 2012, *FracMan*, computer software, version 7.4, FracMan Technology Group.

Gómez, R, Castro, R, Betancourt, F & Moncada, M 2021, 'Comparison of normalized and non-normalized block caving comminution models', *Journal of the Southern African Institute of Mining and Metallurgy*, vol. 121, no. 11, pp. 581–588, https://doi.org/10.17159/2411-9717/1150/2021

Gómez, R, Castro, RL, Casali, A, Palma, S & Hekmat, A 2017, 'A comminution model for secondary fragmentation assessment for block caving', *Rock Mechanics and Rock Engineering*, vol. 50, no. 11, pp. 3073–3084, https://doi.org/10.1007/s00603-017-1267-2

Gomez, R, Castro, RR, Castillo, J, Gómez, R, Castro, RR & Castillo, J 2023, 'Modelamiento de fragmentación durante el flujo gravitacional en minería de Block Caving' (Modeling of fragmentation during gravity flow in block caving operations), in K Suzuki, J Jarufe, M Silva & A Villouta (eds), *1o Congreso Chileno Mecánica de Rocas,* Sociedad Chilena de Mecánica de Rocas, Santiago, pp. 428–439.

Gómez, R, San Martin, C & Castro, R 2025, 'An integrated cellular automata model improves the accuracy of secondary fragmentation prediction', *Applied Sciences*, vol. 15, no. 10, https://doi.org/https://doi.org/10.3390/app15105425

Hekmat, A, Fustos, R, Gomez, R & Vivero, G 2024, 'Estimacion de fragmentacion en mineria subterranea usando inteligencia artificial basada en parametros de perforacion y tronadura' (Fragmentation estimation in underground mining using artificial intelligence and drilling and blasting parameters), in R Castro & R Gomez (eds), *UMining 2024: Tercer Congreso Iberamericano de Minería Subterránea y a Cielo Abierto,* Universidad de Chile, Santiago, pp. 489–501.

Hurtado, J, Pereira, J & Campos, R 2007, *Informe Final Backanalysis De Fragmentación, Minas: Diablo Regimiento* Reno *Y Teniente 4 Sur Tonalita* (Final Report of Fragmentation Back-analysis in mines: Diablo Regimiento, Reno, and Teniente 4 Sur Tonalinta), Nnm-Ico-Geo-Inf No 003, internal report.

Karekal, S, Das, R, Mosse, L & Cleary, PW 2011, 'Application of a mesh-free continuum method for simulation of rock caving processes', *International Journal of Rock Mechanics and Mining Sciences*, vol. 48, no. 5, pp. 703–711, https://doi.org/10.1016/j.ijrmms.2011.04.011

Laubscher, D 2000, 'Drawpoint spacing', *Block Cave Manual*, Julius Kruttschnitt Mineral Research Centre, Indooroopilly.

Laubscher, D, Guest, A, Jakubec, J & Chitombo, G 2017, *Guidelines on Caving Mining Methods: Underlying Concepts*, WH Bryan Mining Geology Research Centre, The University of Queensland, Brisbane.

Laubscher, DH 1994, 'Cave mining-the state of the art', *Journal of the Southern African Institute of Mining and Metallurgy*, vol. 94, no. 10, pp. 279–293.

Laubscher, DH 2000a, 'Primary fragmentation', *Block Cave Manual*, Julius Kruttschnitt Mineral Research Centre, Indooroopilly.

Laubscher, DH 2000b, 'Secondary fragmentation', *Block Cave Manual*, Julius Kruttschnitt Mineral Research Centre, Indooroopilly.

Le-Feaux, R, Castro, R, Cortez, D, Gómez, R & Silva, D 2021, 'A hybrid extraction level layout design for block caving', *Mining Technology*, vol. 131, no. 1, pp. 51–65, https://doi.org/10.1080/25726668.2021.1992980

YuMing, L, Chen, XW, Feng, XL & Ge, QF 2020, 'Design and production practice of block caving in Pulang Copper mine', in R Castro, F Báez & K Suzuki (eds), *MassMin 2020: Proceedings of the Eighth International Conference & Exhibition on Mass Mining*, University of Chile, Santiago, pp. 736–746, https://doi.org/10.36487/ACG_repo/2063_50

Lopez, C, Lopez, E & Garcia, P 2017, '4.8 Modelo KUZ-RAM adaptado a voladuras subterránea', *Manual de Perforación, Explosivos y Voladuras*, Universidad Politecnica de Madrid, Madrid, pp. 1084–1087.

Lorig, LJ & Cundall, PA 2000, A rapid gravity flow simulator.

Marano, G 1980, 'The interaction between adjacent draw points in free flowing materials and it application to mining', *Chamber of Mines Journal*, vol. 22, pp. 25–32.

Merino, L 1986, *Predicting the Size Distribution of Ore Fragments in Block Caving Mines*, Master's thesis, Imperial College, London.

Nedderman, RM 1995, 'The use of the kinematic model to predict the development of the stagnant zone boundary in the batch discharge of a bunker', *Chemical Engineering Science*, vol. 50, no. 6, pp. 959–965, https://doi.org/10.1016/0009-2509(94)00464-3

Ngidi, SN & Pretorius, DD 2010, 'Impact of poor fragmentation on cave management', in Y Potvin (ed.), *Caving 2010: Proceedings of the Second International Symposium on Block and Sublevel Caving*, Australian Centre for Geomechanics, Perth, pp. 593–601, https://doi.org/10.36487/ACG_rep/1002_41_Ngidi

Onederra, I 2004, 'Breakage and fragmentation modelling for underground production blasting applications', *IRR Drilling & Blasting Conference*, IRR, Perth, pp. 1–19.

Paluszny, A & Zimmerman, RW 2017, 'Modelling of primary fragmentation in block caving mines using a finite-element based fracture mechanics approach', *Geomechanics and Geophysics for Geo-Energy and Geo-Resources*, vol. 3, no. 2, pp. 121–130, https://doi.org/10.1007/s40948-016-0048-9

Paredes, P 2022, 'Evaluation of the effect of wider-spaced layouts in recovery for high column block caves', in Y Potvin (ed.), *Caving 2022: Fifth International Conference on Block and Sublevel Caving*, Australian Centre for Geomechanics, perth, pp. 393–416, https://doi.org/10.36487/acg_repo/2205_27

Parsons, J, Kamp, C, Hinton, M & Czyczurko, A 2024, 'B3 cave management during construction and ramp up at New Afton mine', in Daniel Johansson & Håkan Schunnesson (eds), *MassMin 2024: Proceedings of the International Conference & Exhibition on Mass Mining*, Luleå University of Technology, Luleå, pp. 395–408, https://doi.org/10.36487/ACG_repo/2435_C-08

Pierce, M 2010, *A Model for Gravity Flow of Fragmented Rock in Block Caving Mines*, University of Queensland, St Lucia.

Pierce, ME 2019, 'Forecasting vulnerability of deep extraction level excavations to draw-induced cave loads', *Journal of Rock Mechanics and Geotechnical Engineering*, vol. 11, no. 3, pp. 527–534, https://doi.org/10.1016/j.jrmge.2018.07.006

Pierce, M, Weatherley, DK & Kojovic, T 2010, 'A hybrid methodology for secondary fragmentation prediction in cave mines', in Y Potvin (ed.), *Caving 2010: Proceedings of the Second International Symposium on Block and Sublevel Caving*, Australian Centre for Geomechanics, Perth, pp. 567–581, https://doi.org/10.36487/ACG_rep/1002_39_Weatherley-Pierce

Rogers, S, Elmo, D, Webb, G & Catalan, A 2010, 'A discrete fracture network based approach to defining in situ, primary and secondary fragmentation distributions for the Cadia East panel cave project', in Y Potvin (ed.), *Caving 2010: Proceedings of the Second International Symposium on Block and Sublevel Caving*, Australian Centre for Geomechanics, Perth, pp. 425–439, https://doi.org/10.36487/ACG_rep/1002_29_Rogers

Sahupala, HA, Szwedzicki, T & Prasetyo, R 2010, 'Diameter of a draw zone — a case study from a block caving mine, Deep Ore Zone, PT Freeport Indonesia', in Y Potvin (ed.), *Caving 2010: Proceedings of the Second International Symposium on Block and Sublevel Caving*, Australian Centre for Geomechanics, Perth, pp. 633–644, https://doi.org/10.36487/ACG_rep/1002_44_Szwedzicki

Srikant, A, Nicholas, D & Rachmad, L 2004, 'Visual estimation of fragment size distributions in the DOZ block cave', in A Karzulovic & M Alfaro (eds), *Proceedings of Massmin 2004*, University of Chile, Santiago, pp. 286–290.

Stegman, CL, Togtokhbayar, O, Herselman, S & Altankhuu, B 2022, 'Oyu Tolgoi: engineering a Mongolian caving dynasty', in Y Potvin (ed.), *Caving 2022: Proceedings of the Fifth International Conference on Block and Sublevel Caving*, Australian Centre for Geomechanics, Perth, pp. 625–634, https://doi.org/10.36487/ACG_repo/2205_43

Susaeta, A 2004, 'Theory of gravity flow (Part 1)', in A Karzulovic & M Alfaro (eds), *Proceedings of Massmin 2004*, University of Chile, Santiago, pp. 167–172.

Trueman, R, Castro, R & Halim, A 2008, 'Study of multiple draw-zone interaction in block caving mines by means of a large 3D physical model', International Journal of Rock Mechanics and Mining Sciences, vol. 45, no. 7, pp. 1044–1051, https://doi.org/10.1016/j.ijrmms.2007.11.002

Vasquez, E 2026, *Analisis de la Interacción Entre Puntos de Extracción Mediante DEM* (Analysis of the Interaction Between Extraction Points Using DEM), Universidad de Concepcion, Concepcion.

Vivero, G, Hekmat, A, Fustos, R, Díaz, R & Villaseca, F 2024, 'Software basado en IA para la optimización de la tronadura en minería subterránea', in R Castro & R Gómez (eds), *UMining 2024: Tercer Congreso Iberamericano de Minería Subterránea y a Cielo Abierto,* Universidad de Chile, Santiato, pp. 502–515.

Watson, G 1993, *Flow Patterns in Flat Bottomed Silos, PhD thesis,* University of Edinburgh, Edinburgh.

Wilson, AD, Purba, AM & Sjadat, A 2016, 'Progressing cave performance into the later stages of the Deep Ore Zone mine', *Massmin 2016: Seventh International Conference & Exhibition on Mass Mining*, Australasian Institute of Mining and Metallurgy, Melbourne, pp. 285–292.